

Optical properties of perfluorocyclobutyl polymers. III. Spectroscopic characterization of rare-earth-doped perfluorocyclobutyl polymers

Jennifer Gordon and John Ballato

School of Materials Science and Engineering, Center for Optical Materials Science and Engineering Technologies, Clemson University, Clemson, South Carolina 29634

Dennis W. Smith Jr. and Jianyong Jin

Department of Chemistry, Center for Optical Materials Science and Engineering Technologies, Clemson University, Clemson, South Carolina 29634

Received December 23, 2004; accepted February 21, 2005

We present a continuation of two previous studies [J. Opt. Soc. Am. B **20**, 1838 (2003) and J. Opt. Soc. Am. B **21**, 958 (2004)] on the optical characteristics of perfluorocyclobutyl-based polymers. Previously, the spectral dependences of the refractive index and the extinction coefficient have been calculated, and investigations were made into the theoretical and measured attenuation spectra of these polymers. Here, we report on the erbium-doped perfluorocyclobutyl aryl ether polymer 1,1,1-tris(4-trifluorovinyl)oxyphenyl ethane. The absorption and fluorescence spectra are provided, including the Judd–Ofelt parameterization. The Judd–Ofelt parameters are found to be $\Omega_2 = 16.05 \times 10^{-20} \text{ cm}^2$, $\Omega_4 = 3.67 \times 10^{-20} \text{ cm}^2$, and $\Omega_6 = 3.59 \times 10^{-20} \text{ cm}^2$. These results are compared with those for a similar study on erbium-doped poly(methyl methacrylate), and conclusions are drawn concerning the effect of host properties in the 1550 nm region. © 2005 Optical Society of America

OCIS codes: 160.0160, 160.4760, 160.5470, 160.2540, 160.5690, 300.1030, 300.2140, 300.6280.

1. INTRODUCTION

Over the past several decades, polymer optical fibers have garnered increasing interest for a variety of short-haul applications, including local area optical communication networks and other data links such as those in automobiles.^{1,2} The widespread implementation and integration of such systems require the development of polymeric active devices, such as polymer fiber amplifiers and lasers.^{1,3} In silica-based systems, the use of erbium-doped amplifiers is well established, and researchers have sought methods to fabricate the polymer analog to this device, as well as amplifiers using other rare earths for short-haul systems operating in the visible range.^{1,3–6}

Silica-based telecommunications systems operate at 1550 nm, the minimum point of attenuation for this material. Thus, for telecommunications applications, polymers are sought with minimal losses in this wavelength range, making low optical absorption a key parameter in selecting a polymer for polymer optical fiber fabrication. In polymers, optical attenuation results from electronic excited states, fundamental and overtone molecular bond vibrations, and scattering due to local density and composition fluctuations. The most problematic of these are the C–H vibrational absorptions that occur in the region of the 1550 nm telecommunications window. It is well known that substitution of these ions with heavier ones will shift the vibration energies further into the infrared,

thus reducing the attenuation at shorter wavelengths. As a result, much of the recent research into polymer optical fibers has focused on replacing hydrogen with fluorine.⁶

Several fluoropolymers are already commercially available for these applications, including DuPont's fluoroacrylates⁷ and Teflon amorphous fluoropolymers,⁸ Asahi's Cytop,⁹ Dow Chemical's trifluorovinyl ether-based perfluorocyclobutyl (PFCB) polymers,¹⁰ and new PFCB-containing polymers under investigation by Tetramer Technologies.¹¹ Unfortunately, a considerable number of drawbacks remain for many classes of fluorinated polymers, including poor thermal stability, large birefringence, poor solubility in many common solvents, and difficulty in tailoring the refractive index as is needed for core–clad fabrication. PFCB-containing materials offer potential solutions to these concerns, owing to their excellent solution processability, good mechanical and thermal stability, moisture resistance, and easily tailored refractive index by choice of comonomers.^{12,13} Further, the fabrication of PFCB polymers is somewhat novel in that the polymerization proceeds via a noncondensation step growth mechanism with no need for catalysts. Also, the stereochemistry is unbiased with regard to *cis* or *trans* configurations, typically leading to fully amorphous polymers. PFCB chemistry is based on the thermally initiated cyclopolymerization of bi or tri functional aryl trifluorovinyl ethers to form PFCB-containing polymers.^{13–15} This

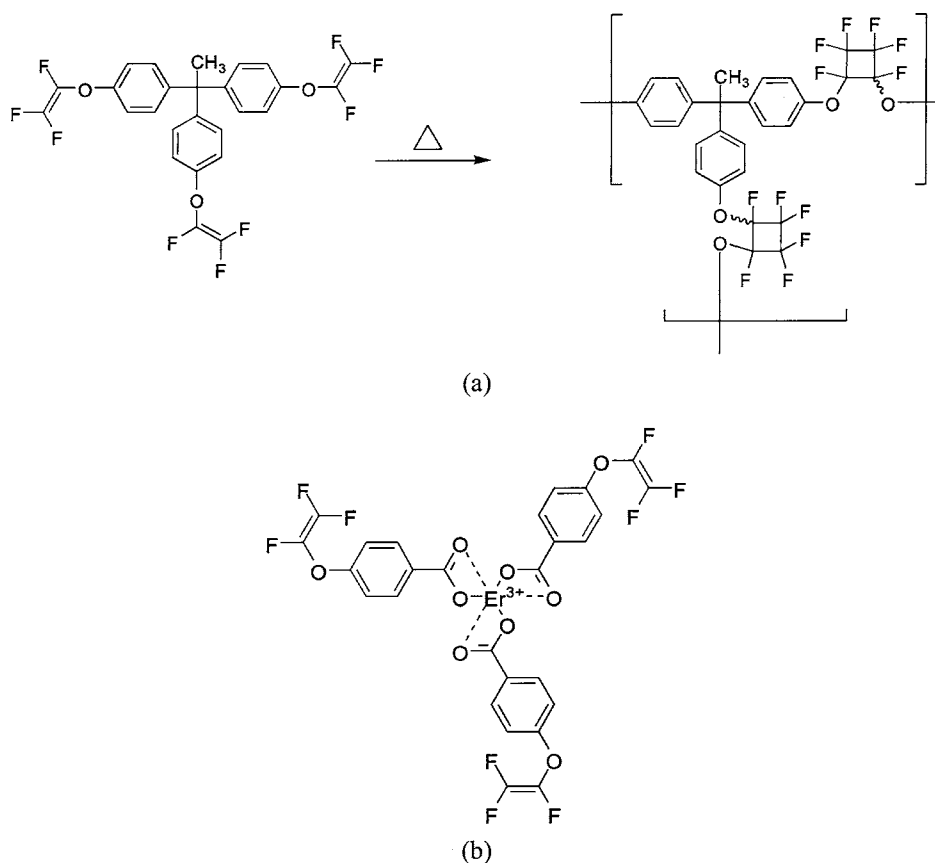


Fig. 1. (a) Polymerization of TVE. (b) Complex used for incorporation of erbium into TVE.

paper focuses on a trifunctional PFCB monomer, 1,1,1-tris(4-trifluorovinyl)oxyphenyl ethane (TVE) [see Fig. 1(a)].

More specifically, the trifunctional PFCB monomer TVE has been doped with erbium through a copolymerization reaction toward the goal of developing active PFCB-based materials. Spectroscopic characterization of the optical properties is carried out through absorption and fluorescence measurements. Judd–Ofelt analysis is then used to determine the spectroscopic properties of erbium-doped PFCB. These results are compared with similar results obtained for erbium-doped poly(methyl methacrylate) (PMMA) samples.

2. EXPERIMENT

A. Sample Preparation

PFCB monomers were prepared as reported previously.^{13–15} The trifunctional monomer TVE was the primary focus of this study, and rare-earth doping was accomplished through copolymerizations with TVE incorporated with erbium (TVE-Er) [see Fig. 1(b)], whose synthesis has been reported elsewhere.¹⁶ Doping levels are stated in terms of the concentration of rare earth to host by weight percent. The average sample size was 1 g.

The appropriate amount of TVE-Er, of the order of 10 mg, was weighed out in a 5 mL glass vial. To this, five drops of ethanol was added. This solution was heated in an oil bath at 80 °C until all the TVE-Er had dissolved. The desired amount of TVE monomer, of the order of 1 g,

Table 1. Absorption Bands Used in the Judd–Ofelt Analysis along with Peak Wavelengths and Refractive Indices of TVE and PMMA at This Wavelength

Excited State	Wavelength (nm)	Refractive Index, PMMA	Refractive Index, TVE
$^4I_{11/2}$	988	NA	1.4899
$^4I_{9/2}$	803	1.4835	1.4933
$^4F_{9/2}$	659	1.4836	1.4982
$^4S_{3/2}$	547	1.4838	1.5050
$^2H_{11/2}$	523	1.4838	1.5071
$^4F_{7/2}$	490	1.4839	1.5106

was then added to the vial. The mixture was capped, again heated in an oil bath at 80 °C, and mixed for approximately 5 min. The vial was then uncapped and placed in a vacuum oven at room temperature. A small amount of nitrogen was fed into the oven to create a slight positive pressure, and the oven was set to 90 °C. While the oven was heating up, the solution was degassed, and the ethanol was removed through repeated cycles of purging with nitrogen and pulling vacuum. The oven was then held at 150 °C for 24 h under a positive nitrogen pressure. At this point, the oven was turned off and allowed to slowly cool to room temperature. The sample could then be removed from the vial. Undoped samples for spectroscopic comparison were prepared by using the same procedure, without the addition of the dopant or ethanol solution.

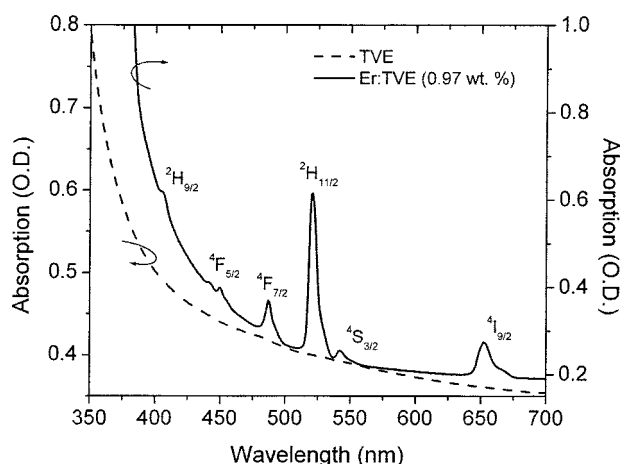


Fig. 2. UV-visible region of absorption spectrum of erbium-doped TVE. Absorptions are from the $^4I_{15/2}$ ground state. O.D., optical density.

PMMA samples were fabricated for the purposes of a comparative study. The dopant used in this paper was Resolve-Al ErFOD, erbium tris(6,6,7,7,8,8,8-heptafluoro-2,2-dimethyl-3,5-octanedionate), purchased from Aldrich in powder form with a purity of 99+ % (Aldrich, St. Louis, Mo.). One can accomplish doping of PMMA by simply dissolving the powder directly into the monomer. Methyl methacrylate and *tert*-butyl peroxide (radical initiator) also were purchased from Aldrich. *N*-butyl mercaptan (chain transfer agent) was purchased from Acros (Acros, Morris Plains, N.J.). Methyl methacrylate, the desired percentage of erbium complex, 0.22 vol. % *tert*-butyl peroxide, and 0.22 vol. % *n*-butyl mercaptan were combined in a glass vial, sonicated for approximately 20 min, and then placed inside a glass tube. The open end of the tube was used to provide a constant nitrogen pressure. This was heated in an oil bath at 90 °C for approximately 24 h. The tubes were then opened, placed in a vacuum oven, and heated for three days at 120 °C at approximately 500 Torr. After this, the polymer was removed from the glass tube. Once the rods were fully formed, they were ground and polished to obtain rods with smooth faces appropriate for optical characterization.

B. Spectroscopic Characterization

We obtained optical absorption data at room temperature by using a PerkinElmer Lambda 900 UV/Vis/NIR spectrometer (PerkinElmer, Wellesley, Mass.). We evaluated the data by using PerkinElmer's UV WinLab Lambda 900 software. Scans were taken at a rate of 100 nm/min with a slit size of 2 nm in the near-IR region and 1 nm in the UV-visible region.

We measured near-IR luminescence from the erbium-doped TVE by using 400 mW of a 980 nm laser diode source and a SPEX Fluorolog II (Horiba Jobin Yvon, Edison, N.J.). We collected fluorescence with 0.5 nm resolution by using a Hamamatsu InGaAs detector (Hamamatsu, Hamamatsu City, Japan).

3. DATA ANALYSIS

The electronic energy states are labeled in the form $^{2S+1}L_J$, referred to as *LS* or Russell-Saunders coupling.

Here, *S* represents the total spin quantum number, *L* represents the total orbital angular momentum, and *J* provides the total angular-momentum quantum number for that level. Russell-Saunders notation applies to weakly coupled systems, such as the rare earths, where the outerlying 5*s* and 5*p* electrons shield the 4*f* states from the influences of the ligand field, making the transition free-ion-like.^{17,18}

Technically *f-f* transitions are parity forbidden, but the ligand field admixes 5*d*, 5*g*, etc., electronic character and yields partially allowed transitions guided by the following selection rules.¹⁸⁻²⁰

Electric dipole: $\Delta S=0$, $\Delta L=\pm 1$, $|\Delta L|$, $|\Delta J|\leq 6$, unless *J* or *J'*=0 when $|\Delta J|=2, 4, 6$.

Magnetic dipole: $\Delta S=\Delta L=0$, $|\Delta J|\leq 1$ (except $0\leftrightarrow 0$), $|\Delta l|=0$.

Electric quadrupole: $\Delta S=0$, $|\Delta L|$, $|\Delta J|\leq 2$ (except $0\leftrightarrow 0$, $0\leftrightarrow 1$), $|\Delta l|=0$.

Vibronic $\Delta J=0, \pm 2$.

For the erbium-doped TVE samples, six absorption bands between 490 and 988 nm were chosen for evaluation of the three Judd-Ofelt parameters.^{21,22} Peaks at higher energies were not used owing to the obscuring of these peaks from host scattering contributions to the spectra. In the PMMA samples, the peak at 988 nm could not be resolved, so only five bands were included in the analysis. In both cases, the absorption band centered around 1535 nm has been purposefully left out of the analysis, as will be explained later in this paper. This peak will be discussed in terms of how well the calculated values for the Judd-Ofelt parameters allow the prediction of the line strength of this peak. Table 1 lists the absorption bands used in this study with their peak wavelengths and refractive indices. As the Judd-Ofelt theory is widely employed and well established, only a brief background is given here.

The line strengths for an electric dipole transition, S^{ed} , between states $^{2S+1}L_J\leftrightarrow^{2S'+1}L'_J$, can be expressed as²⁰

$$S^{\text{ed}}[(S,L)J;(S',L')J'] = \sum_{t=2,4,6} \Omega_t |\langle (S,L)J || U^{(t)} || (S',L')J' \rangle|^2,$$

where the $U^{(t)}$ -matrix elements are the doubly reduced unit tensor operators relating to the rare earth to be

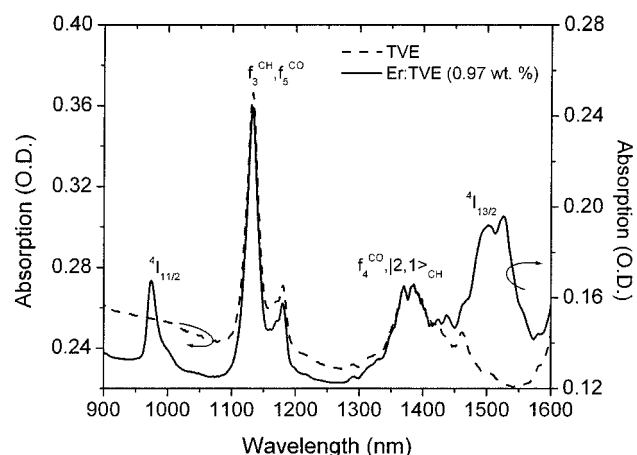


Fig. 3. Near-IR region of absorption spectrum of erbium-doped TVE. Absorptions are from the $^4I_{15/2}$ ground state.

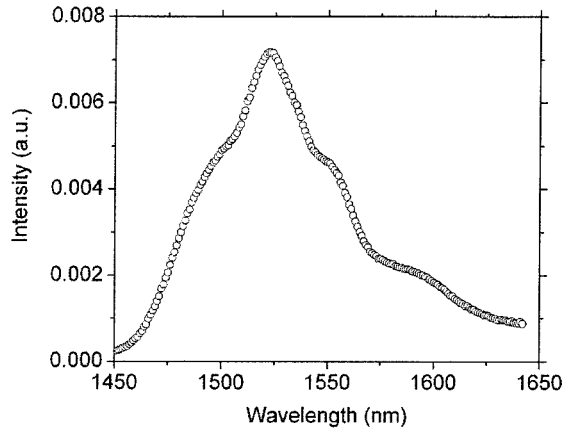


Fig. 4. Emission from the ${}^4I_{13/2}$ to the ${}^4I_{15/2}$ ground state in 0.97 wt. % erbium-doped TVE, 980 nm pump.

evaluated and are independent of the host material. The Judd–Ofelt parameters, Ω_t , are host-dependent factors that provide information into the transition probability and host bonding environment.^{23,24}

Magnetic dipole line strengths, S^{md} , can be similarly expressed as²⁰

$$S^{\text{md}}[(S,L)J;(S',L')J'] = \left(\frac{eh}{4\pi mc} \right)^2 | \langle (S,L)J || L + 2S || (S',L')J' \rangle |^2,$$

where e is the charge on an electron, h is Planck's constant, m is the mass of an electron, and c is the speed of light. S^{md} is not affected by the local environment of the rare earth and thus is generally considered to be a constant for any rare-earth transition, unlike S^{ed} , which is strongly host dependent.²⁰ Generally, the probabilities for magnetic dipole transitions are much less than those for electric dipole transitions; and their contribution to the total line strength is typically insignificant. However, in some cases they may contribute significantly. The ${}^4I_{15/2}$ to ${}^4I_{13/2}$ absorption in erbium at 1535 nm is an example of this.²⁵ Thus, for completeness, the magnetic dipole contribution to this transition has been subtracted from the total line strength for this peak to give the electric dipole line strength.

The measured electric dipole line strengths can then be calculated from the integrated absorbance²⁰:

$$\int k(\lambda) d\lambda = \frac{8\pi^3 e^2 \lambda_{\text{avg}} N K}{3ch(2J+1)n^2} (\chi_{\text{ed}} S^{\text{ed}} + \chi_{\text{md}} S^{\text{md}}),$$

where $k(\lambda)$ is the absorption coefficient at the wavelength λ ; λ_{avg} is taken as the mean wavelength of the peak measured; N is the rare-earth ion concentration in ions/cm³; K is 1.0 g cm³ s⁻² statcoulomb⁻² and necessary for the line strengths S^{ed} and S^{md} to be dimensionless; χ_{ed} is the electric dipole local field correction, which equals $n(n^2+2)^2/9$, where n is the refractive index at the wavelength λ ; χ_{md} is the magnetic dipole local field correction, which equals n^3 ; and all other variables are as previously defined.

4. RESULTS AND DISCUSSION

Figure 2 provides the absorption spectrum of erbium-doped TVE in the UV–visible range along with an undoped reference sample. It can be observed that the doped sample suffers from higher scattering losses than the undoped sample at higher energies. This is likely due to the formation of dopant clusters at the relatively high concentrations used here, approximately 1 wt. %. These concentrations were chosen to ensure strong absorption lines that could be easily observed. However, this relatively high concentration inevitably also leads to concentration quenching, hence to low lifetime, and also may reduce the accuracy of the computed Judd–Ofelt parameters.

Figure 3 shows the near-IR spectral range for the same sample and an undoped reference sample. In this figure, absorptions resulting from the overtone vibrations of the C–O and C–H bonds have also been labeled.²⁶ The peaks in the range of 1100 to 1200 nm, labeled as f_3^{CH} , f_5^{CO} , result from the third harmonic of the C–H vibration and the fifth harmonic of the C–O bond, respectively. A broad peak in the range of 1300 to 1500 nm, labeled as f_4^{CO} , $|2,1\rangle_{\text{CH}}$ is attributed to the fourth harmonic of the C–O bond and the combination bands of the first and second harmonics of the C–H bonds.

The emission at 1550 nm from the ${}^4I_{13/2}$ level down to the ${}^4I_{15/2}$ ground state is shown in Fig. 4. The emission is weaker than anticipated as evidenced by the reasonably high pump power required. By Raman spectroscopy, TVE is found to have a phonon energy in the range of 1600 cm⁻¹ likely due to C–H bond vibrations.²⁶ Compared with silica, this is a relatively large phonon energy. Therefore, it can be inferred that nonradiative processes likely dominate the relaxation from the ${}^4I_{13/2}$ level down to the ground state, resulting in a weak emission of 1550 nm light. This assertion was corroborated in part by measurement of the radiative lifetime, found to be approximately 50 μs , which is within the temporal resolution of the measurement and significantly shorter than desired.⁴

The absorption spectra of the doped sample shown in Figs. 2 and 3 were used to perform Judd–Ofelt analysis on the doped TVE. Similar analysis was performed on a 0.75 wt. % erbium-doped PMMA sample. The resulting values for the Judd–Ofelt parameters, along with the root-mean-square error, are given in Table 2. Table 3 gives the measured electric dipole line strengths as compared with the calculated line strengths. In most cases, the agreement is reasonable, within the 10%–20% accuracy typically expected from the Judd–Ofelt phenomenology.

The relatively large values of Ω_2 result from the asymmetry of the rare-earth ion site and are indicative of the presence of covalent bonding between the rare-earth ion

Table 2. Judd–Ofelt Parameters for Erbium-Doped TVE and PMMA

Parameter	PMMA+0.75 wt. % Er ³⁺	TVE+0.97 wt. % Er ³⁺
$\Omega_2 \times 10^{-20}$ cm ²	60.04	16.05
$\Omega_4 \times 10^{-20}$ cm ²	4.10	3.67
$\Omega_6 \times 10^{-20}$ cm ²	2.99	3.59
rms error $\times 10^{-20}$	0.218	0.210

Table 3. Comparisons of the Observed and Calculated Values for S^{ed} in TVE and PMMA

Excited State	PMMA		TVE	
	$S_{\text{observed}}^{\text{ed}} \times 10^{-20}$	$S_{\text{calculated}}^{\text{ed}} \times 10^{-20}$	$S_{\text{observed}}^{\text{ed}} \times 10^{-20}$	$S_{\text{calculated}}^{\text{ed}} \times 10^{-20}$
${}^4I_{13/2}$	0.24	5.93	5.29	5.41
${}^4I_{11/2}$	NA	NA	1.87	1.75
${}^4I_{9/2}$	0.52	0.80	0.42	0.78
${}^4F_{9/2}$	3.66	3.55	3.70	3.59
${}^4S_{3/2}$	0.61	0.67	0.64	0.72
${}^2H_{11/2}$	46.00	46.00	13.64	13.64
${}^4F_{7/2}$	2.42	2.48	2.80	2.62

and the surrounding ligand.⁴ Clearly, the results show a strongly asymmetric site in the doped PMMA material and a more symmetric site in the TVE system. The calculated values for the Judd–Ofelt parameters for TVE are within the range of other values published for organic media and show the rare-earth ion site in this material to still be somewhat asymmetric.^{4,27–29}

As mentioned earlier, the absorption band from the ground state to the ${}^4I_{13/2}$ level was not included in the analysis. However, this peak has been included in the results shown in Table 3 for the purposes of discussion. A comparison of the electric dipole line strengths calculated from the spectroscopic results and that which would be calculated from the Judd–Ofelt parameters for this peak provides some instructive results.

For the PMMA sample, the line strength calculated by using the Judd–Ofelt parameters is too large by approximately an order of magnitude as compared with the experimentally observed value. It is well known that vibrations from C–H bonds occur near the 1550 nm region. This absorption should be expected to mask part of the Er^{3+} absorption peak, much like the effects of scattering on the shorter wavelength transitions. Thus, the integrated absorption of the 1535 peak is less than expected owing to that part that cannot be measured because it overlaps the C–H absorptions. The primary reason for investigating fluorinated polymers such as TVE is the expectation that absorption losses in the 1550 nm wavelength range will be decreased by one's replacing C–H bonds with C–F bonds. Thus, it would be expected that the calculated line strength for this peak in TVE would better agree with that observed than for a host polymer such as PMMA. Indeed, it can be seen in Table 3 that the calculated value is now much closer to the experimental value, being off by only approximately 10%, as compared with the PMMA value, which is off by an order of magnitude.

These results not only confirm that TVE has lower losses than PMMA in the 1550 nm region, but they should also serve as a note of caution for others using Judd–Ofelt analysis to evaluate hydrocarbon-based polymers. The matrix elements are not the only factor influencing the measured line strength of a transition. Losses in the range of a rare-earth transition must also be considered.

However, there is another factor that contributes to this. As a result of the peaks that have been chosen to de-

termine the Judd–Ofelt parameters, there is only one, the hypersensitive absorption from the ground state to the ${}^2H_{11/2}$ level, that determines the value of Ω_2 . The large line strength of this transition resulting from the asymmetry of the site is the reason for the large value of Ω_2 . This also contributes to the overestimation of the ${}^4I_{13/2}$ peak as it is also dependent on the value of Ω_2 . Also, because the TVE site is more symmetric than the site in PMMA, this effect is more pronounced in the doped PMMA. This explanation alone, however, is not enough to explain the significant overestimation of the ${}^4I_{13/2}$ line strength in the PMMA sample. Absorption factors also contribute.

5. CONCLUSION AND FUTURE RESEARCH

1,1,1-tris(4-trifluorovinyloxy)phenyl ethane has been doped with 0.97 wt. % erbium. Absorption and emission spectra have been obtained from these samples. The absorption spectra have been used to perform Judd–Ofelt analysis. The Judd–Ofelt parameters were calculated for erbium-doped TVE and are $\Omega_2=16.05 \times 10^{-20}$, $\Omega_4=3.67 \times 10^{-20}$, and $\Omega_6=3.59 \times 10^{-20} \text{ cm}^2$. Further, similar analysis has been performed on PMMA erbium-doped samples, and the results are compared. The results indicated that the rare-earth ion site is more symmetric in the PFCB system than in the PMMA system and also showed the effect of absorptions on the Judd–Ofelt analysis.

Ultimately, it is desirable to incorporate rare earths into linear members of the PFCB family so that fiber amplifiers can be drawn from these materials. Thus, the primary focus of future efforts will be the preparation of doped PFCB preforms for these purposes. In addition, more ligands appropriate for use in PFCB materials are under investigation that may yield more promising results.

ACKNOWLEDGMENTS

The authors acknowledge Matt Dejneka (Corning, Incorporated) for spectroscopic measurements. Financial support of the 3M Corporation (Junior Faculty Awards to J. Ballato and D.W. Smith, Jr.), the Defense Advanced Research Projects Agency (grants N66001-01-1-8938 and N66001-03-1-8900 for the Laboratory for Advanced Pho-

tonic Composites), and the U.S. Department of Commerce (through grant 99-27-07400 through the National Textile Center).

J. Ballato, the corresponding author, can be reached by e-mail at jballat@clemsun.edu.

REFERENCES

1. A. Tagaya, Y. Koike, T. Kinoshita, E. Nihei, T. Yamamoto, and K. Sasaki, "Polymer optical fiber amplifier," *Appl. Phys. Lett.* **63**, 883–884 (1993).
2. T. Freeman, "Plastic optical fibre tackles automotive requirements," *Fibers.org*, June 14, 2004, <http://fibers.iop.org/articles/news/6/6/7/1>.
3. S. Xiaohong, M. Hai, D. Ning, X. Aifang, H. Jun, Z. Qijin, Y. Min, Z. Zebo, and X. Jianping, "Using spectra analysis and scanning near-field optical microscopy to study Eu doped polymer fiber," *Opt. Commun.* **208**, 111–115 (2002).
4. L. R. Dalton, C. Koeppen, S. Yamada, G. Jiang, and A. F. Garito, "Rare-earth organic complexes for amplification in polymer optical fibers and waveguides," *J. Opt. Soc. Am. B* **14**, 155–162 (1997).
5. A. J. Kenyon, "Recent developments in rare-earth doped materials for optoelectronics," *Prog. Quantum Electron.* **26**, 225–284 (2002).
6. L. H. Slooff, A. Van Blaaderen, A. Polman, G. A. Hebbink, S. I. Klink, F. C. J. M. Van Veggel, D. N. Reinhoudt, and J. W. Hofstraat, "Rare-earth doped polymers for planar optical waveguides," *J. Appl. Phys.* **91**, 3955–3980 (2002).
7. L. Eldad and L. Shacklette, "Advances in polymer integrated optics," *IEEE J. Sel. Top. Quantum Electron.* **6**, 54–68 (2000).
8. P. R. Resnick and W. H. Buck, "Teflon AF amorphous fluoropolymers," in *Modern Fluoropolymers*, J. Scheirs, ed. (Wiley, 1997), pp. 397–419.
9. N. Sugiyama, "Perfluoropolymers obtained by cyclopolymerization and their applications," in *Modern Fluoropolymers*, J. Scheirs, ed. (Wiley, 1997), pp. 541–555.
10. D. A. Babb, B. Ezzell, K. Clement, W. Richey, and A. Kennedy, "Perfluorocyclobutane aromatic ether polymers," *J. Polym. Sci. Part A Polym. Chem.* **31**, 3465 (1993).
11. E. Wagener, Tetramer Technologies, 657 S. Mechanic Street, Pendleton, S.C. 29670, <http://www.tetramertechologies.com> (personal communication, 2003).
12. J. Ballato, S. Foulger, and D. W. Smith, Jr., "Optical properties of perfluorocyclobutyl polymers," *J. Opt. Soc. Am. B* **20**, 1838–1843 (2003).
13. D. W. Smith, Jr., S. Chen, S. M. Kumar, J. Ballato, C. Topping, H. V. Shah, and S. H. Foulger, "Perfluorocyclobutyl copolymers for microphotonics," *Adv. Mater.* **14**, 1585–1589 (2002).
14. D. W. Smith, Jr., and D. A. Babb, "Perfluorocyclobutane aromatic polyethers. Synthesis and characterization of new siloxane-containing fluoropolymers," *Macromolecules* **29**, 852–860 (1996).
15. D. A. Babb, H. Boone, D. W. Smith, Jr., and P. Rudolf, "Perfluorocyclobutane aromatic ether polymers. III. Synthesis and thermal stability of a thermoset polymer containing triphenylphosphine oxide," *J. Appl. Polym. Sci.* **69**, 2005–2012 (1998).
16. J. Jin, J. Barden, A. R. Neilson, J. Gordon, J. Ballato, and D. W. Smith, Jr., "Trifluorovinylether functionalized semi-fluorinated lanthanides (III) complexes: synthesis and characterization," *Polym. Mater. Sci. Eng.* **91**, 812–813 (2004).
17. G. H. Dieke, *Spectra and Energy Levels of Rare-Earth Ions in Crystals*, H. M. Crosswhite and H. Crosswhite, eds. (Interscience, 1968).
18. R. D. Peacock, *The Intensities of Lanthanide f-f Transitions*, Vol. 22 of Structure and Bonding (Springer-Verlag, 1975), p. 84.
19. W. T. Carnall, P. R. Fields, and K. Rajnak, "Electronic energy levels in the trivalent lanthanide aquo ions. I. Pr³⁺, Nd³⁺, Pm³⁺, Sm³⁺, Dy³⁺, Ho³⁺, Er³⁺, and Hm³⁺," *J. Chem. Phys.* **49**, 4424–4442 (1968).
20. M. Dejneka, E. Snitzer, and R. E. Riman, "Blue, green, and red fluorescence and energy transfer of Eu³⁺ in fluoride glasses," *J. Lumin.* **65**, 227–245 (1995).
21. B. R. Judd, "Optical absorption intensities of rare-earth ions," *Phys. Rev.* **127**, 750–761 (1962).
22. G. S. Ofelt, "Intensities of crystal spectra of rare-earth ions," *J. Chem. Phys.* **37**, 511–520 (1962).
23. S. Tanabe, "Optical transitions of rare earth ions for amplifiers: How the local structure works in glass," *J. Non-Cryst. Solids* **259**, 1–9 (1999).
24. S. Tanabe, "Rare-earth-doped glasses for fiber amplifiers in broadband telecommunication," *C. R. Chim.* **5**, 815–824 (2002).
25. A. Kaminskii, *Crystalline Lasers: Physical Processes and Operating Schemes*, (CRC Press, 1996), p. 235.
26. J. Ballato, S. Foulger, and D. W. Smith, Jr., "Optical properties of perfluorocyclobutyl polymers. II. Theoretical and experimental attenuation," *J. Opt. Soc. Am. B* **21**, 958–967 (2004).
27. R. Sosa Fonseca, M. Flores, R. Rodriguez, J. Hernandez, and A. Munoz, "Evidence of energy transfer in Er³⁺-doped PMMA–PAAc copolymer samples," *J. Lumin.* **93**, 327–332 (2001).
28. K. Kuriki, S. Nishihara, Y. Nishizawa, A. Tagaya, Y. Koike, and Y. Okamoto, "Spectroscopic properties of lanthanide chelates in perfluorinated plastics for optical applications," *J. Opt. Soc. Am. B* **19**, 1844–1848 (2002).
29. Z. Zheng, H. Liang, H. Ming, Q. Zhang, and J. Xie, "Optical transition probability of the Er³⁺ Ion in Er(DBM)₃ phen-doped poly(methyl methacrylate)," *Opt. Commun.* **233**, 149–153 (2004).